Prepared for:

RIKZ/National Institute for Coastal and Marine Management

Diagnostic studies NOURTEC

Comparison between Torsminde and Terschelling shoreface nourishments

Report on model investigation

May 1996

delft hydraulics

Diagnostic studies NOURTEC

Comparison between Torsminde and Terschelling shoreface nourishments

A.J.H.M. Reniers and J.A. Roelvink

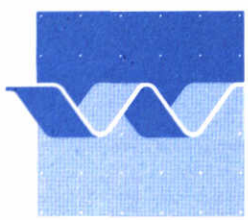

delft hydraulics

Contents

List of figures

1 Introduction

In the following the modelling concepts used for the Thorsminde and the Terschelling shoreface nourishments are discussed. Both nourishments, aimed at stabilising the retreating coastline, were part of an EU-funded project, "NOURTEC". A third project site was situated at Norderney, Germany. The modelling is performed with the process-based profile model UNIBEST-TC. This was previously done for the Terschelling case, Roelvink and Meijer, 1995, which showed that the model could be calibrated to reproduce important changes in the bathymetry using a realistic parameter setting. The same procedure is followed in the Thorsminde case, which is described in Chapter 2, to further verify the model and to examine the validity of the parameter settings found for the Terschelling case.

The modelling of the profile development is based on cross-shore transport gradients only, which is a valid approximation in the case of alongshore uniformity. This may be the case for the autonomous area and part of the nourishment area. Obviously this is not true at the nourishment heads, where alongshore variations in the bathymetry induce complex wave patterns and corresponding 2D current patterns. These effects are not represented by the present modelling approach. However, the alongshore variation in the longshore sediment transport at the nourished and autonomous profiles can be used to estimate the overall migration rate of the nourishment. This is described in Chapter 3.

Finally a synthesis of model results and measurement data is given in Chapter 4. An overview of phenomena and mechanisms observed in the data and simulated by the models is presented. The combination of both is used to reach some specific conclusions regarding the behaviour of shore face nourishments and the required modelling approach.

2 Modelling of the Thorsminde case

2.1 Introduction

In the period between March 29 and June 10 1993, a beach and shore face nourishment were deployed two km apart near Thorsminde (Denmark), both with a length of approximately one km and a sand volume of 250 000 m^3. The life expectancy of both nourishments is in the order of three years. This chapter describes the modelling approach and modelling results used in the study on the morphodynamic behaviour of the shoreface nourishment. The model is used in its socalled diagnostic mode where the objective is to simulate the profile development within the measuring period. The results can be used in a discussion on the modelling approach for shoreface nourishments. General info on the data required for the modelling study is described in Section 1.2. The schematisation and corresponding numerical aspects are given in Section 1.3. A discussion on the results follows in Section 1.4 and some conclusions in Section 1.5.

2.2 Data description

Bathymetry

The bathymetry is obtained from detailed surveys with a 100 m alongshore spacing in the survey lines, starting at crest of the dune toward approximately 13 m water depth. The estimated standard deviation (error) in the measurements is about .1 m. Just after the deployment surveys were performed monthly, weather permitting. After the initial changes in bathymetry, the survey interval was increased to three months.

The survey data of 10 June 1993 was interpolated on a rectangular grid with an alongshore spacing of 50 metres and cross-shore spacing of 15 metres. The nearshore bathymetry near Thorsminde is characterised by a (multiple) bar system, see upper panel of Figure 1, where the dark colours indicate the trough and light colours the crest of the bars. Note that not all of the bathymetry is shown, but attention is focused on the area near the shoreface nourishment. There is some considerable alongshore variability present, with the exception of the area down South which has a clear multiple barred profile. The shoreface nourishment was deployed seaward of the outer bar at a water depth of MSL -4 m. The berm height at the nourishment site after deployment is in the order of 2.5 m, which is denoted by the lightly coloured area offshore.

The following bathymetry, see middle panel Figure 1, was obtained from the survey information 162 days after the nourishment was deployed. It shows the changes in the vicinity of the nourishment, which apparently is becoming less steep at the offshore side. Furthermore the trough between the nourishment and the water line is becoming shallower. The alongshore variability at the two ends of the nourishment has increased. Southward the nourishment berm has more or less attached itself to the outer bar, indicating a strong southward directed sediment transport pattern. Northward the berm height has decreased, i.e. a flattening of the nourishment head. Behind the nourishment, sediment deposits are visible, not unlike the initial stage of a tombolo effect. This is confirmed by the erosion-accretion patterns shown in the upper panel of Figure 2, which displays the changes in bed-level after 162 days.

The final bathymetry, see lower panel of Figure 1, was obtained 254 days after the initial deployment. The nourishment berm is now fully attached to the outer bar further south, where the whole bathymetry has become much more alongshore uniform. North of the nourishment there is still considerable alongshore variability in the bathymetry. Behind the nourishment the erosion has increased compared to the previous case, see middle panel of Figure 2, displaying the erosion accretion patterns between the second and third survey. The total erosion accretion patterns are shown in the lower panel of Figure 2, with local changes in the bed level varying between plus and minus 2 metres.

Two profiles were to be selected for the modelling: an autonomous profile and a profile representative for the shoreface nourishment (see Table 1), with a total modelling time span of 254 days. The profiles were selected on the criterion that the conditions in the vicinity of the bottom profiles are more or less alongshore uniform. With the predominant wave direction being from the North-West, an autonomous bottom profile due North of the nourishment areas would be best. However, North of the nourishments little information on the bathymetry is available, so instead a profile far south of the nourishments was selected, at line 21860. For convenience the beach profile at the shoreface nourishment area was kept at the position previously used by the Danish Coastal Authority (Design report of the three NOURTEC test sites, 1994, which will be referred to as DR94 in the following), i.e. line 21860.

Description	Line	Date	D_{50}	
shoreface	21860	10-06-1993	0.45	
		22-11-1993	0.45	
		22-02-1994	0.45	
autonomous	21680	10-06-1993	0.35	
		22-22-1993	0.35	
		22-02-1994	0.35	

Table 1 Selected profiles

The profiles used for the model computations were obtained by averaging over three adjacent profiles to eliminate small local disturbances (e.g. due to measurement errors). A visual check was used to verify the alongshore uniformity in the vicinity of the selected profiles. The profiles, see Figure 3, typically have a plane offshore slope of 1:100 followed by a bar-trough region. Closer to the shore, the bottom profile steepens considerably, varying from 1:15 to 1:25. From bottom samples, see Scientific and Technical Progress Report, 1994, (referred to in the following as PR94), it follows that the grain size distribution varies in the cross-shore direction for each transect, becoming coarser further onshore, in correspondence with the steep beach profiles near the water line.

The profile development at the shoreface nourishment, lower panel Figure 3, confirms the earlier described behaviour obtained from the total bathymetric data (Figures 1 and 2). The offshore slope is becoming milder, accompanied by the strong erosion at the inshore side of the nourishment and accretion further toward the water line. The response of the autonomous profile, upper panel Figure 3, is much milder, displaying an offshore migration of the outer bar.

Wave and water level data

Wave height and direction are obtained from a directional wave rider, located 2 km North of the survey area, at the 20 m depth contour. Data is recorded for 20 min. with a sampling interval of three hours. A second measurement was obtained from the combined current-pressure gauge, which is located in the survey area at a depth of 12 meters. Unfortunately this instrument was not functioning reliably and the results have not been used in this study. Wave height, period and direction, obtained from the wavec, are shown in Figure 4. It shows the presence of two small storms at the end of the period in an otherwise mild wave climate. The time series for the wave period is discontinuous around T = 150 days and at the very end. Filling the gap with measurement data obtained from the combined current velocity pressure sensor was not possible because the device did not operate reliably. The correction of the wave period time series is therefore based on the following. A plot of the wave height-wave period combinations, see upper panel Figure 5, shows the presence of both sea and swell waves. This means there is no unequivocal relation between wave height and period. Given the fact that the wave climate is governed predominantly by sea waves, we have used the following relation to obtain the corresponding wave period:

$$T_p = \alpha \sqrt{H_{rms}}$$

where α is a coefficient which was fitted to the data (see also Figure 5). The resulting time series are shown in Figure 6. Wave directions in Figure 4 are given with respect to the North. This shows that the predominant direction during this period was from the North-West. A coordinate transformation was used to obtain the wave direction with respect to the shore normal, as shown in Figure 6.

The half-hour mean water level is recorded at Thorsminde, which is approximately 1 km South of the survey area. A second measurement station is located 5 km North of the Survey area. For both stations a six minute mean is used, with a sampling interval of 15 min. Water levels are given with reference to DNN. There is a gap in the mean water level measurements around T = 200 days (see lower panel Figure 4). A comparison with the mean water levels measured near Thorsminde shows a good match, see lower panel Figure 5, and was used to complete the time series, as can be seen in Figure 6.

Sedimentological data

The representative D_{50} for each transect, see also Table 1, is taken from the bottom samples obtained in the bar-trough regions (PR94), given the fact that these are the most dynamic. Next a simple formulation is used to relate the D_{50} inversely proportional to the local water depth (Roelvink and Meijer, 1995), thus varying the D_{50} across the profile, becoming coarser onshore.

2.3 Modelling aspects

The coordinate system originates approximately 1400 m offshore at a water depth of 12 m, x being positive onshore along the coast normal.

The grid spacing is given in Table 2, starting with a coarser grid offshore toward a finer grid spacing in the surf zone where stronger gradients are expected. It was verified that using this grid spacing gave no loss of accuracy compared to a finer grid.

From (m)	To (m)	Number of cells	Grid size (m)
-1395	-1095	6	50
-1095	- 895	8	25
- 895	- 55	84	10
- 55	0	11	5

Table 2 Grid size distribution

The time series for the required wave and water level boundary conditions are given with a three hour interval. The morphological time step in the numerical model was set at 1 day which was verified to be without loss of accuracy in the predicted morphological development of the bottom profiles.

As mentioned previously, the bottom profiles become very steep near the water line and beyond. From bottom samples it is known that locally the beach is made up of coarse sand including pebbles. At present the profile model is not fit to cope with such materials. The fact that the transport of such materials is small under normal conditions, the upper part of the beach was modelled as a fixed bottom.

2.4 Results

As mentioned previously, the model was run in its diagnostic mode only, where the comparison of model results and measurements is based on the profile development after 254 days. Note that there is no data available to verify and calibrate the hydrodynamic part of the model. Based on previous model exercises only the following parameters were varied in the sensitivity runs:

wave breaking parameter γ;
wave breaker delay represented by λ;
slope effect inversely proportional to the angle of repose $\tan\varphi$.

The variation in parameter values and corresponding run-codes are given in Table 3.

Run code	Profile	λ	γ	$\tan\varphi_1$	$\tan\varphi_2$	$x\varphi_1$	$x\varphi_2$
202	autonomous	2	0.60	0.1	0.1	900	1200
203	autonomous	2	0.60	0.3	0.1	900	1200
204	autonomous	2	0.60	0.3	0.05	900	1200
205	autonomous	2	0.50	0.3	0.05	900	1200
206	autonomous	1	0.60	0.3	0.05	900	1200
301	nourished	2	0.60	0.3	0.05	900	1200
304	nourished	2	0.60	0.1	0.05	600	1200
307	nourished	2	0.60	0.15	0.05	700	1300

Table 3 Parameter setting sensitivity runs

Autonomous profile

Cross-shore variation of the slope effect was used, varying linearly between its value $\tan\varphi_1$ at position $x\varphi_1$ and $\tan\varphi_2$ at position $x\varphi_2$. Note that the slope effect had to be increased, i.e. a decrease in the angle of repose, toward the water line in order to obtain the best results for the autonomous profile development, which is contrary to the experience obtained with the Terschelling case. An angle of repose similar to the Terschelling case, $\tan\varphi = 0.1$, led to a strong onshore sediment transport near the outer bar, quickly filling the trough (see upper panel Figure 7), resulting in an overall smooth profile. Increasing the angle of repose, $\tan\varphi = 0.3$, led to a significantly improved prediction of the outer bar behaviour (see lower panel Figure 7). Further decreasing of the nearshore value of $\tan\varphi$ to 0.05 showed good correspondence with the profile development near the water line (see upper panel Figure 8). The required cross-shore distribution of $\tan\varphi$ is likely to be correlated to the strong variation in the medium grain size and the corresponding steep slopes. Part of that was compensated by introducing the depth dependence in the D_{50}. However, the fact that the sediment consists of mixed materials such as sand, gravel and pebbles is not incorporated in the present sediment transport model.

Once the slope effect was established other parameters could be varied. A wave breaker delay of $\lambda = 2$ proved to give good results, compare upper panel of Figure 8 and lower panel of Figure 9. Increasing the λ parameter value further proved to give a negligible effect. The wave breaker parameter γ was optimised to be 0.6 (compare upper panel Figure 8 and upper panel Figure 9.

For the autonomous profile a good match with the measurements was obtained in run 205 (see Figure 8). The modelled offshore motion of the outer bar corresponds well to the measurements. The measurements show a slightly increased steepening of the upper part of the beach. Still the changes are small and the fixed bottom approach can be seen to be valid. The overall correspondence is good.

The 'measured' averaged sediment transport was obtained from the following balance:

$$\frac{\partial S_x}{\partial x} + \frac{\partial z_b}{\partial t} = 0$$

taking the cross-shore sediment transport at the offshore boundary to be equal to its computed counterpart, S_{c0}, the cross-shore distribution of the sediment transport is given by:

$$S_x = \int_0^{x_s} \frac{z_b(t_1) - z_b(t_2)}{\Delta t} dx_s + S_{c0}$$

where t_1 and t_2 refer to the times at which the bottom profiles where measured. The resulting averaged sediment transport is shown in the lower panel of Figure 8. Note that the transport is predominantly directed onshore. It is also apparent there is a positive trend indicating the presence of an alongshore gradient in the transport which is eroding the profile. This is in accordance with the overall observed trends. The comparison with the computed transport, also shown in Figure 8, compares favourably with the measurements with maximum differences in the order of twice the computed transport. The positions of maximum and minimum transports coincide well.

Nourished profile

As a start the parameter settings obtained with the modelling of the autonomous profile where used to predict the behaviour of the nourished profile, see upper panel Figure 10. The nourishment develops into two bars propagating offshore. The amplitude of the outer bar grows continuously becoming very steep, unlike the measurements.

The nourishment was deployed at a water depth of approximately 4 m. The bed level changes in the autonomous profile at this water depth were negligible and thus could not be calibrated. In the autonomous case an angle of repose of .3 was required to model the behaviour of the outer bar. Decreasing the overall slope effect results in an improved correspondence with the measurements, though the overall profile is becoming too smooth. A next step is to adapt the slope effect further offshore only to dampen the strong growth observed in the nourished profile. The angle of repose now varies linearly from its offshore value to a value of .3 at the position of the outer bar as observed in the autonomous profile, i.e. x = 900 m. Next the angle of repose decreases again to its nearshore value. This concept was tried for a number of offshore values of the angle of repose. The best results are obtained for run 307, as shown in Figure 11. The offshore slope of the outer bar at the nourishment is becoming milder corresponding to the measurements. However, the predicted offshore motion of the outer bar is not present in the measurements. The measured sediment transport again indicates the presence of an alongshore transport gradient. If this is taken into account, the overall correspondence between predictions and measurements is fair.

2.5 Conclusions

The bathymetric development, see Figures 1 and 2, showed the strong response of the nourishment to the hydrodynamic conditions, with a rapid development of a more alongshore uniform bathymetry dominated by the southward directed sediment transport flux. It also showed the presence of sometimes strong alongshore variability in the bathymetry. Further down south, the bathymetry becomes more alongshore uniform.

The modelling of the autonomous profile development at Thorsminde required the introduction of a fixed beach due to the fact that the sediment transport of mixed materials is not included at present. Once introduced, the profile development simulation was satisfactory, showing a good correspondence between measured and modelled cross-shore distributions of the sediment transport rates. Compared to the Terschelling case, the parameter setting for $\tan\varphi$ was different, decreasing in value towards the shore line as opposed to an increasing value. This is most likely correlated to the coarse material and corresponding steep slopes. Note that ϕ is used as a calibration coefficient and not as the actual angle of repose. The settings for the wave breaker delay proved to be the same as in the Terschelling case, supporting the concept. The profile development seemed marginally influenced by the presence of the nourishment further North, given the presence of the alongshore gradient in the sediment transport.

The parameter setting for the angle of repose as obtained for the autonomous situation proved to be inadequate for the nourished profile, resulting in strong growth of the outer bar which was not observed in the measurements. This was improved by decreasing the angle of repose further offshore. Overall the match between the modelled and measured development of the nourished profile was less good compared to the autonomous profile. Part of this may be explained by the rather strong alongshore variability which was present in the bathymetry in the vicinity of the nourishment (see Figure 1) and corresponding alongshore gradients. This was apparent in the observed connecting of the nourishment berm with the outer bar further south.

3 Longshore transport analyses

The longshore dispersion and translation of shoreface nourishments such as at Terschelling and at Thorsminde are certainly influenced by non-local flow effects, typical 2D current patterns and complex wave patterns. These effects can not be represented by models which assume longshore uniformity. However a "far-field" estimate can be made of the overall migration rate of a nourishment by comparing the undisturbed and disturbed cross-shore distributions of the longshore transport. The idea is that the difference in longshore sediment transport is caused by the presence of the nourishment. The migration rate of the nourishment is than given by:

$$C_y = dy/dt = \frac{\int_{x_2}^{x_1} S_d - S_u \, dx}{\int_{x_1}^{x_2} Z_d - Z_u \, dx}$$

Where x_1 and x_2 represent the cross-shore section of the nourishment, the subscripts d and u stand for disturbed and undisturbed respectively. S represents the alongshore sediment transport and Z the bed level.

In Figure 12 the undisturbed and disturbed profiles at Thorsminde are shown in the upper panel, and the longshore transport averaged over the 254 day period in the lower panel.

The result for the nourishment section (between 660 m and 830 m in the figure) is a migration rate of approx. 150 m over the 254-day period, which is in reasonable agreement with the observed stretching in southward direction.

In Figure 13 the same is shown for the Terschelling case. The migration rate of the nourishment is now 110 m in the 120-day winter period of the simulation. This simulation does not include wind-driven currents; in Figure 14, these are included in the computation, which leads to an increase in the transports by approximately 15%. The general shape of the transport pattern is not affected significantly.

An important finding for the Terschelling case is the dramatic decrease of the longshore transport along the inner bar. This may well be an explanation for the observed height of the inner bar in the nourishment area, especially at the western end, and may lead to strong erosion at the eastern part.

The conclusion of these analyses must be that longshore effects are certainly relevant for the behaviour of shoreface nourishments, and must be taken into account in a thorough manner. The present computations and data analyses can only yield preliminary estimates of the eventual effects. In future cases, the use of area modelling to identify various problem spots is strongly recommended.

4 Synthesis of model results and measurement data

In this chapter an overview is given of phenomena and mechanisms which are observed in the data and simulated by the models, and an effort is made to make use of the combination of both. We will do this in a "top-down" fashion, starting at the large scale patterns and going down to small-scale processes.

Long-term morphodynamics

Long-term yearly profile surveys for the Terschelling case show a clear cyclic behaviour of the sand bars in cross-shore direction, with a period in the order of 10 years. Compared to the transport rates involved in the cross-shore motion of the bars, the cycle-averaged transport rates responsible for long-term erosion or accretion are small. Given the fact that the bars are almost shore-parallel, the dominant mechanism must be cross-shore transport. This also leads to the conclusion that the observed structural erosion is largely a function of longshore transport gradients.

A behaviour like this can occur when the transport pattern follows the bar pattern in such a way, that seaward transport peaks are at bar crests and landward peaks are in the troughs. On average, this may result in near-zero net transport with seaward moving bars.

In the model exercises with UNIBEST-TC it has been shown that such behaviour may be explained by a combination of cross-shore mechanisms such as undertow, streaming, wave asymmetry and bound long waves. Critical model components are the wave breaker delay and bottom slope effect. The first of these gives rise to an instability mechanism without which no bars are formed, and the second is essential in controlling the growth of the bars.

Medium-term cross-shore morphodynamics

Detailed comparisons have been carried out between measured and simulated profile behaviour over a 120-day winter period for the Terschelling site and for a 254-day period at the Thorsminde site. Some parameters in the UNIBEST-TC model were calibrated within a reasonable range. A common sensitive parameter in both cases was the bottom slope effect. Values for a bed slope parameter between 0.05 and 0.30 were found to produce reasonable results. Clearly, much research is need before this range can be narrowed down without local calibration. Especially in the Thorsminde case the wide range of sediment fractions poses problems to the modelling. In both cases there is a tendency of coarsening with decreasing water depth; however, this is much more extreme in the Thorsminde case. Separate modelling of sediment fractions will be necessary to enable real progress.
The alongshore spatial scales for Terschelling and Thorsminde differ. The latter is relatively short compared to the cross-shore scales, which resulted in a strong alongshore variability. The cross-shore behaviour is therefore contaminated by the alongshore variability.
Though the length scales for Terschelling were considerably longer, the effect of alongshore variability in the cross-shore morphodynamics could not be neglected either.

Medium-term longshore morphodynamics

From the bathymetric measurements at both sites (PR 94) a net longshore motion of the nourishments can be observed (see also Figure 1), in the order of 100-200 m per year. This can be explained by the increase of sediment transport rates over the nourishments as reproduced by the model. On the updrift side this leads to erosion and on the downdrift side to accretion, hence the net displacement.
Beside the net motion of the nourishments there is a considerable longshore dispersion which is related to the gross longshore transports in both directions. This is evident in the early behaviour of the Terschelling nourishment, but also very clear in the Thorsminde case looking at the bathymetric development (PR 94).

Especially in the Thorsminde case the length of the nourishment is relatively small compared to the cross-shore scales which results in complex horizontal (2D) circulation patterns. Therefore, a purely cross-shore or longshore model schematisation is likely to be problematic. The combination of a cross-shore modelling approach with a depth-averaged 2D approach focusing on non-uniform longshore effects can therefore be effective. Ideally, these features are combined into a (quasi-) 3D model.

Cross-shore distribution of longshore transport

A striking feature in the transport computations for both sites is the fact that the longshore transport rates are largest at the seawardmost bar. This transport is dominated by storm conditions since not much happens under normal conditions at these locations. The observed development in longshore direction of the nourishment at Thorsminde indeed shows large changes at the location of the nourishment and outer bar.

The longshore transport in the nearshore zone is affected significantly by the presence of a nearshore nourishment. This may lead to important local erosion or accretion. In the Thorsminde case, the scales of the nourishment are such that it is difficult to distinguish between these effects and purely cross-shore effects.

Tide- and wind-driven currents

These currents were studied extensively at the Terschelling site [Bakker, 1995]. The cross-shore distribution of the tidal velocities is reasonably well described by the simple assumption of a constant gradient. The longshore wind-driven currents are modelled quite well by the UNIBEST-TC model, even though this only takes into account locally generated wind-driven currents.

For the prediction of net longshore transports it is important to take into account the wind component, since this has a strong eastward bias.

Wave-driven currents

According to the model computations wave-driven current effects dominate both longshore and cross-shore transports. Investigations to compare the model results with the (limited) observations of wave-driven currents are under consideration.

Wave decay

The amount of dissipation of wave energy over the breaker bars is of great importance for the cross-shore distribution of currents and transports. In the Terschelling case the wave model in UNIBEST-TC has been calibrated against the large amount of data [Bakker, 1995]. Although standard settings of the Battjes-Janssen [1978] type model produced reasonable results, some improvements were found to be possible for a slightly modified setting. This setting has been applied in subsequent analyses.
The concept of "breaker delay" was introduced during this study after new data had become available in the framework of the LIP-11D test programme. Since the data from NOURTEC were
not suitable for testing the concept the LIP-11D data set was applied. The resulting formulation leads to much more realistic profile behaviour, while the overall wave dissipation remains relatively unchanged.

Long wave effects

The long wave motions at the Terschelling site have been studied at Utrecht University by Ruessink [1995]. The data and model analyses support the hypothesis that much of the incoming long wave energy is dissipated at the beach. This and the fact that the LF energy spectrum is broad-banded preclude the formation of strong standing wave patterns. The role of long waves in forming bars is therefore limited, although there is a significant effect on cross-shore transport due to the correlation between short wave energy and (bound) long waves.

Wave asymmetry

The asymmetry of the orbital motion, expressed as the third odd velocity moment, may be somewhat overestimated by the model due to the short-crestedness of the wave field. Investigations into this for the Terschelling site are being considered.

Sediment transport

Investigations into the important mechanisms of sediment transport are still ongoing at Utrecht University. Contrary to earlier preliminary findings, there now appears to be a significant role of the oscillatory part of the suspended sediment flux (Personal communication Ruessink and Houwman). In the present model set-up, this oscillatory part is neglected for the suspended flux, although it is taken into account in the bed-load transport formulation. In view of this it is likely that the model results, which have been calibrated against the morphodynamic behaviour, overestimate the bed-load transport while underestimating the onshore component of the suspended load.

Sedimentology

Both in the Terschelling case and in the Thorsminde case, significant sediment sorting effects have been observed (Guillén and Hoekstra, 1996). At Terschelling, the sorting was shown to re-establish quickly after the nourishment. At the Thorsminde site, the sorting was even stronger. In the present modelling, the observed trends were simply reproduced in the model, but not predicted by it. There is a lack of knowledge about the effect of grain size and grading on both the transport rate and on the bed slope effect.

Conclusions

The combination of integral models (e.g. N-line models), detailed process models (e.g. UNIBEST-TC) and the measurement data in the NOURTEC project has increased our understanding of the relevant processes. The importance of effects on the nourishments caused by the processes discussed above have been assessed. This has allowed improvements, e.g. breaker delay, presentation of grainsize distribution as function of depth and validation of the overall model (morphodynamic behaviour). In addition, major weak spots have been identified, e.g. grain sorting and bed-slope effect. Therefore we conclude that the application of process-based modelling in combination with monitoring can be useful to predict the effects of nourishments.

References

Bakker, R., 1995: NOURTEC; Verification of the UNIBEST-TC model. Report RIKZ/OS-95.133x, Rijkswaterstaat, National Institute for Coastal and Marine Management, The Hague.

Battjes, J.A. and J.P.F.M. Janssen, 1978: Energy loss and set-up due to breaking in random waves. Proc. 16th Int. Conf. on Coastal Eng., Hamburg, ASCE, pp. 569-587.

Design report of the three NOURTEC test sites, 1994.

Guillén, J. and P. Hoekstra, 1996: The "equilibrium" distribution of grainsize fractions and its implications for cross-shore sediment transport: conceptual model. In press at Marine Geology.

Roelvink, J.A. and Th.J.G.P. Meijer, 1995: Diagnostic studies NOURTEC, Calibration of the profile model UNIBEST-TC. DELFT HYDRAULICS report H1698, June 1995.

Ruessink, B.G., 1995: On the origin of infragravity waves in the surf zone of a dissipative multiple bar system. Proc. Coastal Dynamics'95 Conf., Gdansk, Poland.

Scientific and Technical Progress Report June 1993 - June 1994, 1994.

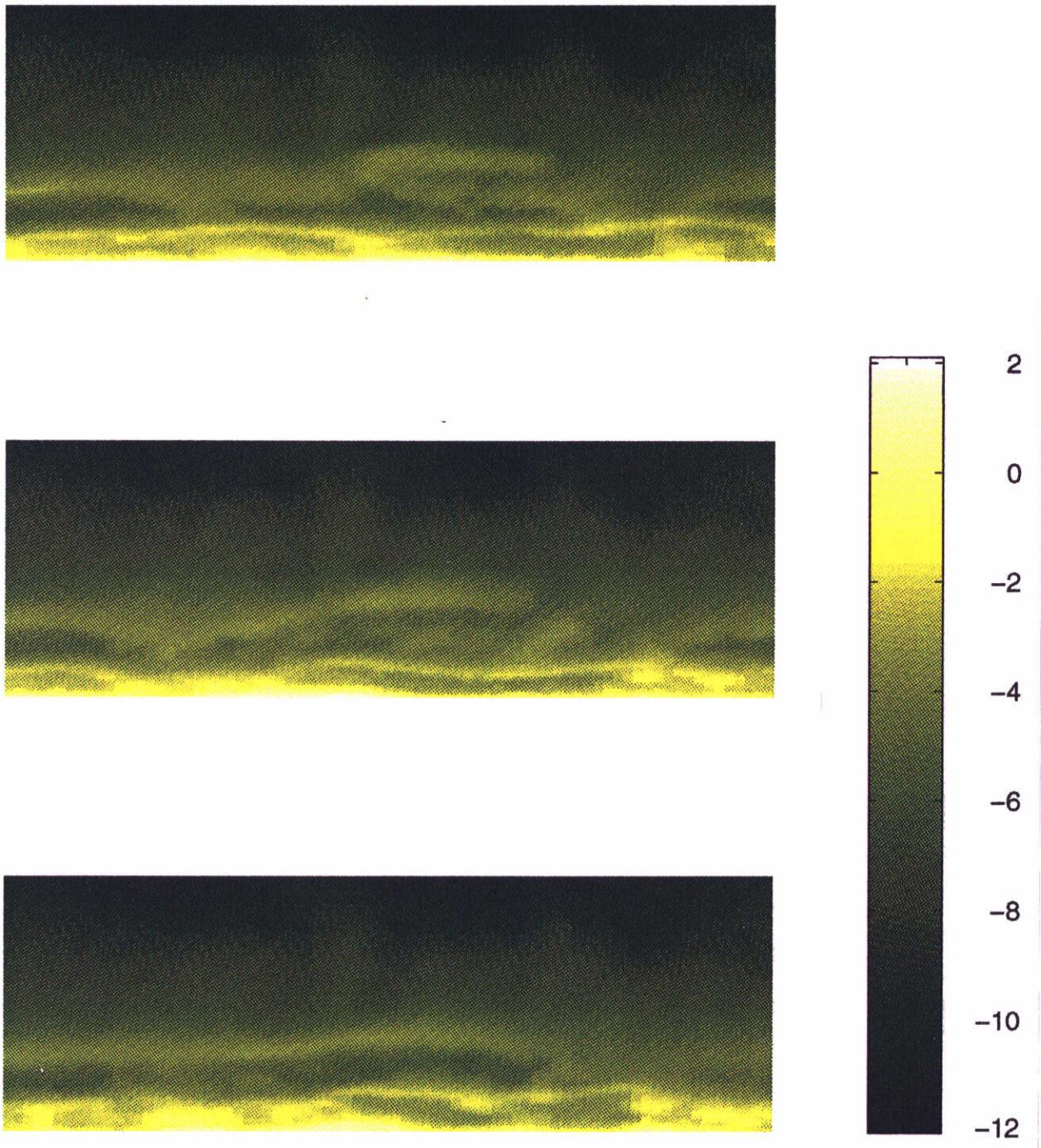

Bathymetric development

upper panel: just after nourishment

middle panel: 162 days, lower panel: 254 days

NOURTEC

Scale 1 : 35000

DELFT HYDRAULICS

H1698

Fig 1

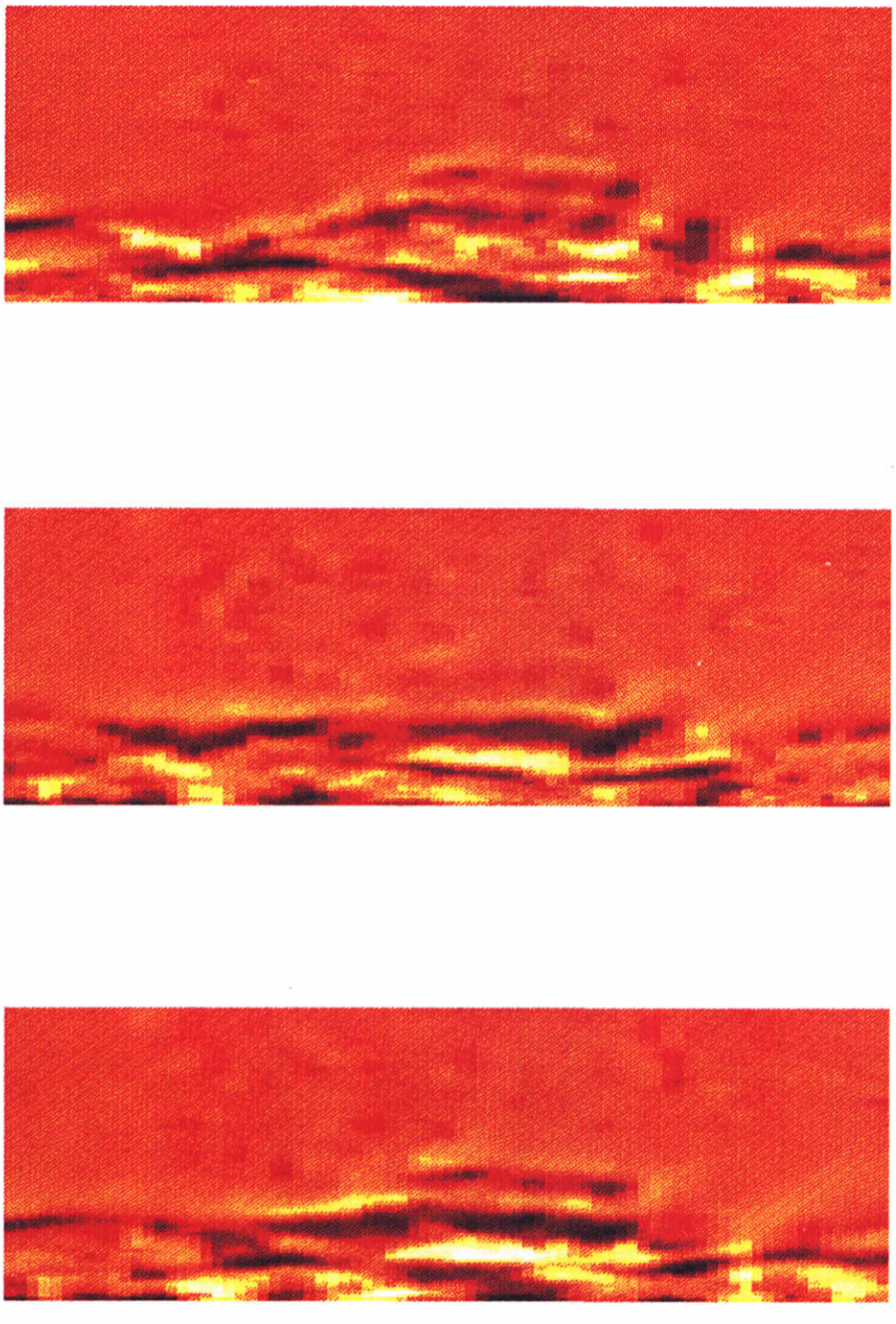

Bedlevel changes upper panel: first 162 days
middle panel: following 92 days
lower panel: complete period of 254 days

NOURTEC

Scale 1 : 35000

DELFT HYDRAULICS

H1698

Fig 2

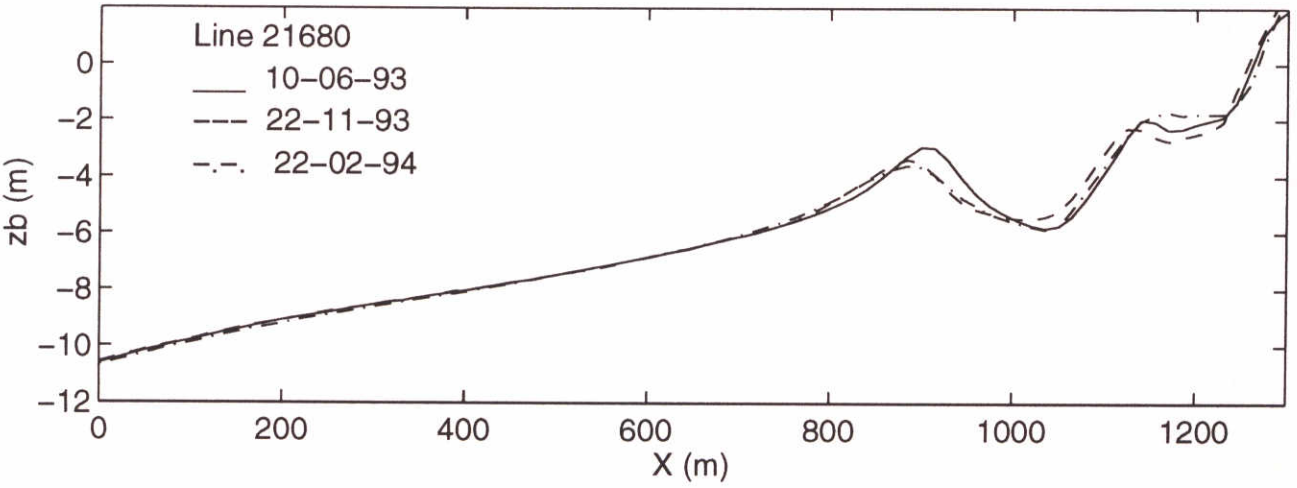

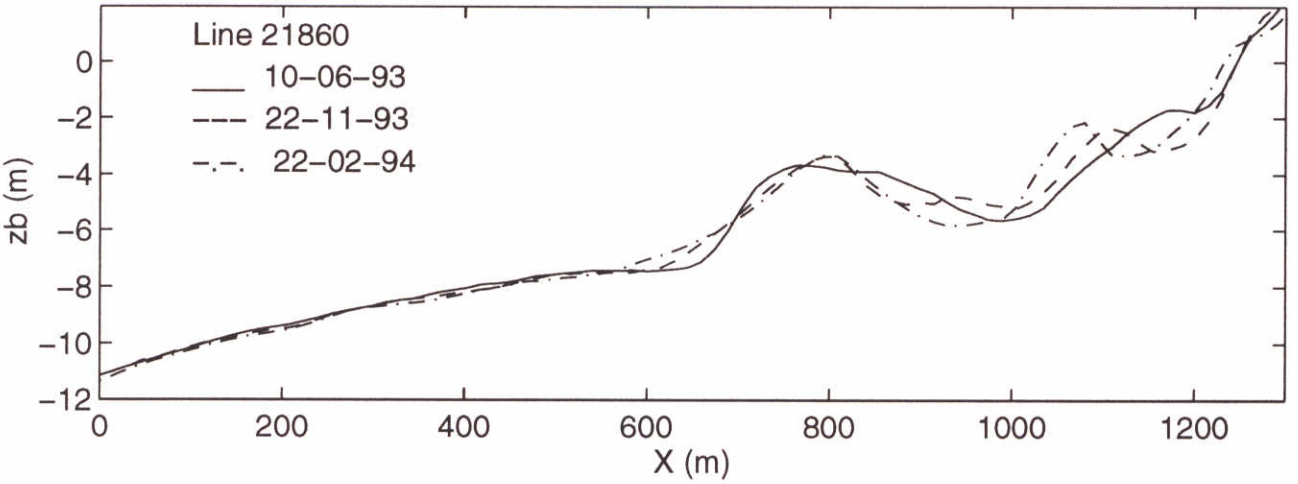

Bottom profiles
upper panel: autonomous profile
lower panel: nourishment profile

NOURTEC

DELFT HYDRAULICS

H1698

Fig 3

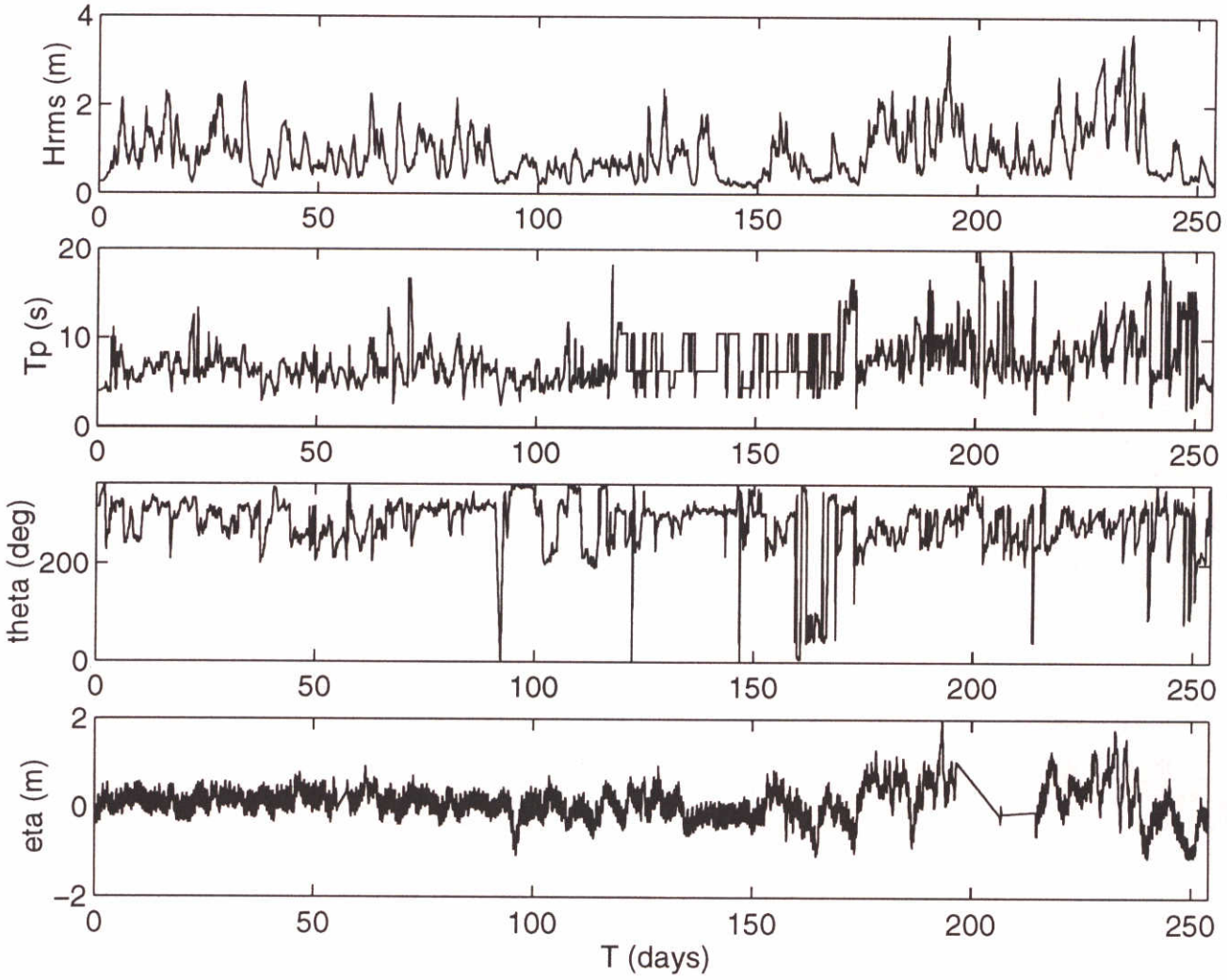

Wave and water level data	NOURTEC	
DELFT HYDRAULICS	H1698	Fig 4

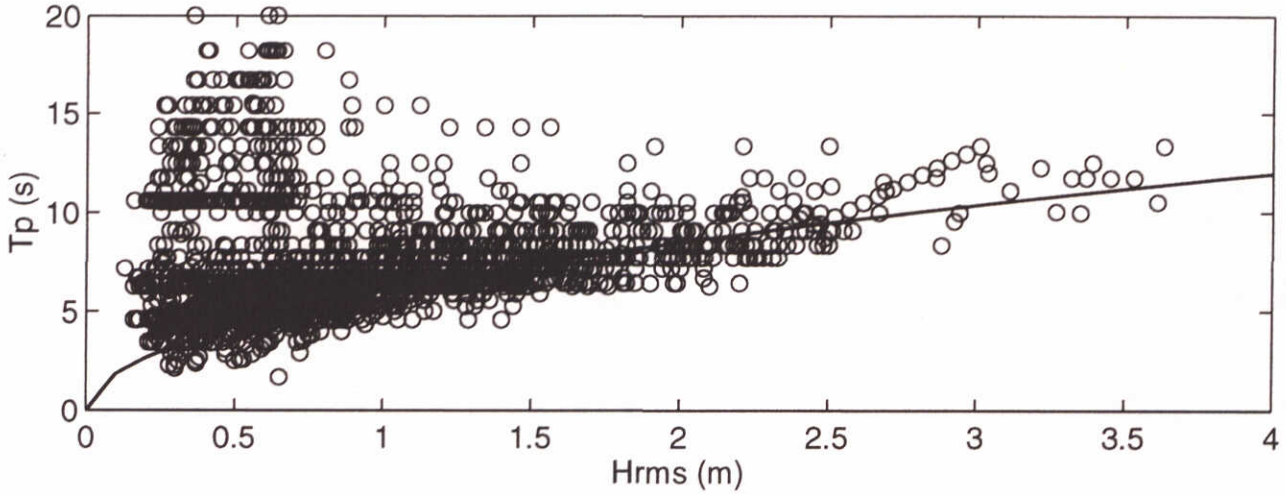

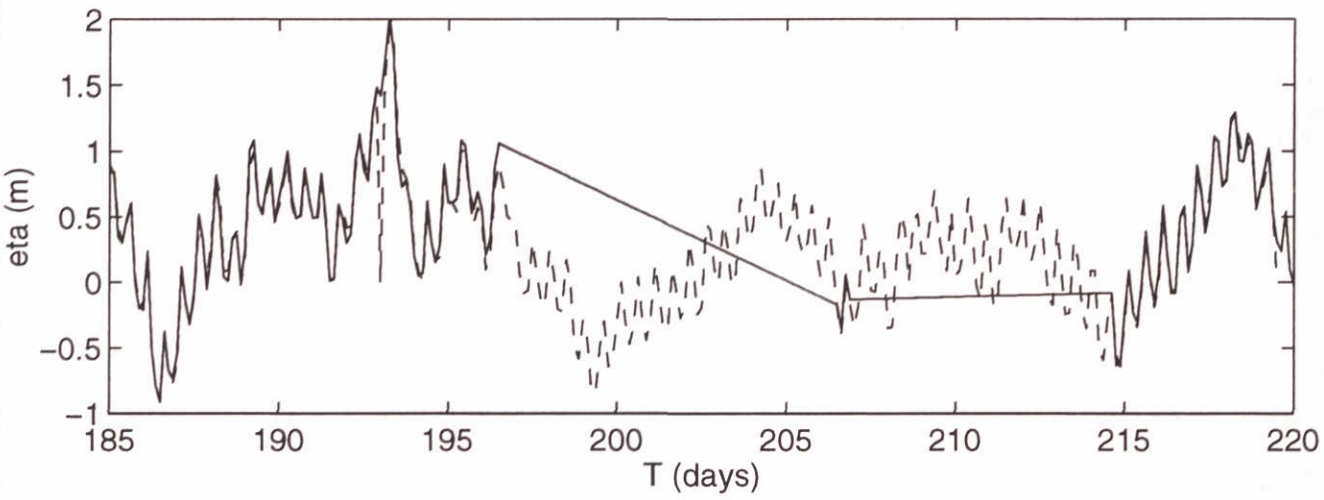

Additional data

upper panel: Hrms-Tp relation

lower panel: comparison measurements water level

NOURTEC

DELFT HYDRAULICS

H1698

Fig 5

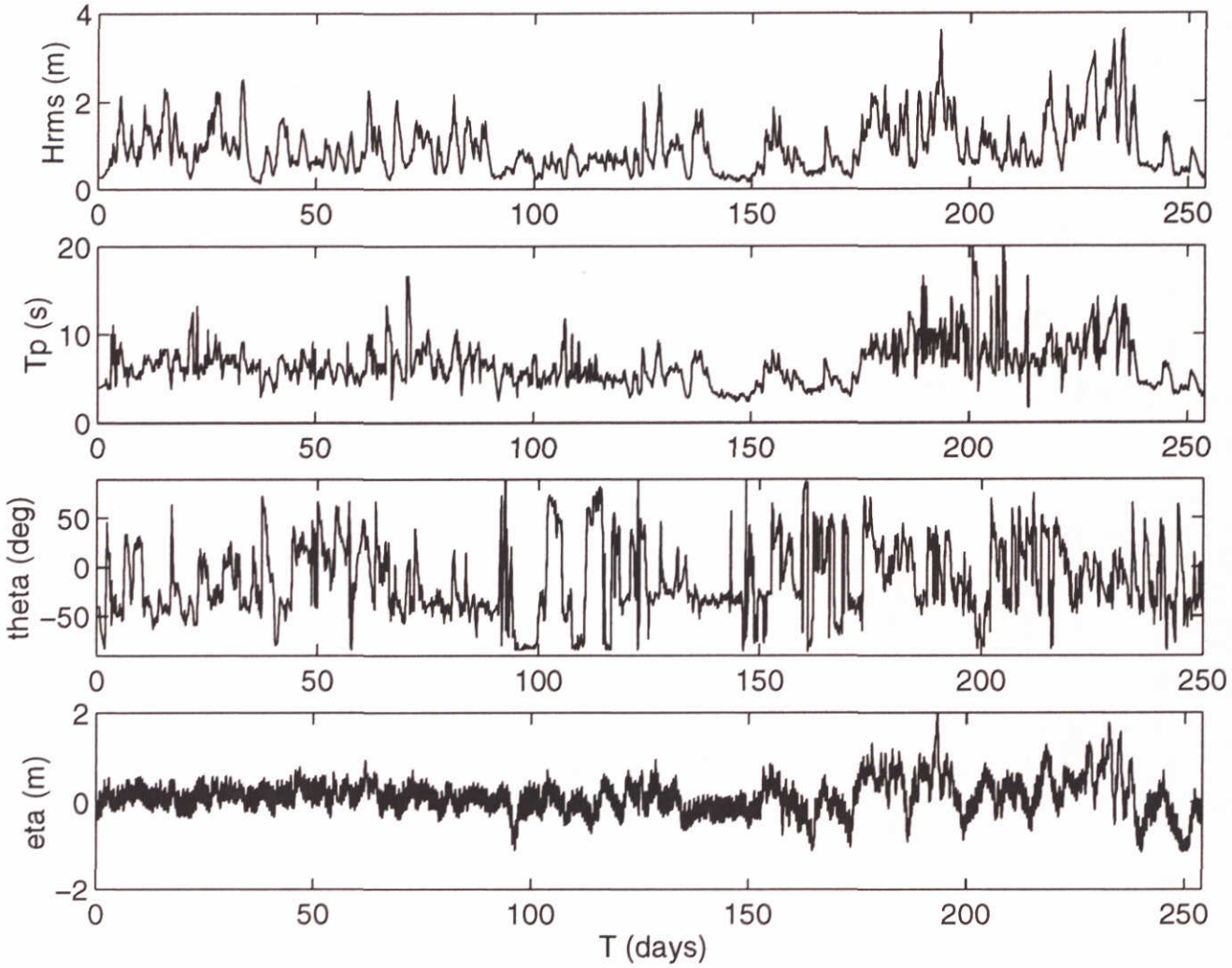

Wave and water level data

with additional data

NOURTEC

DELFT HYDRAULICS

H1698

Fig 6

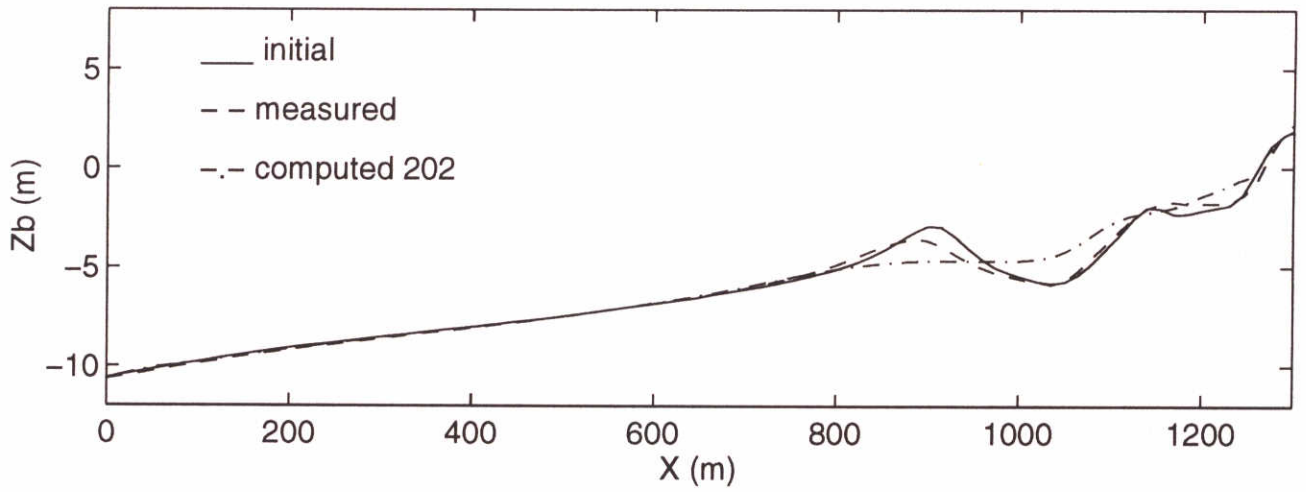

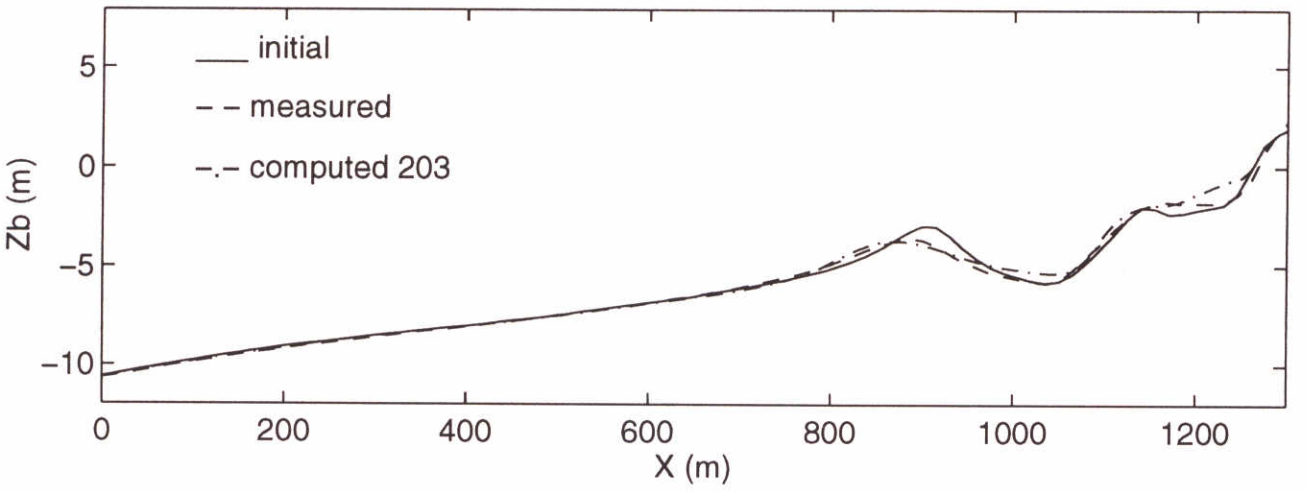

Comparison model vs. measurements
slope effect
autonomous profile after 254 days

NOURTEC

DELFT HYDRAULICS

H1698

Fig 7

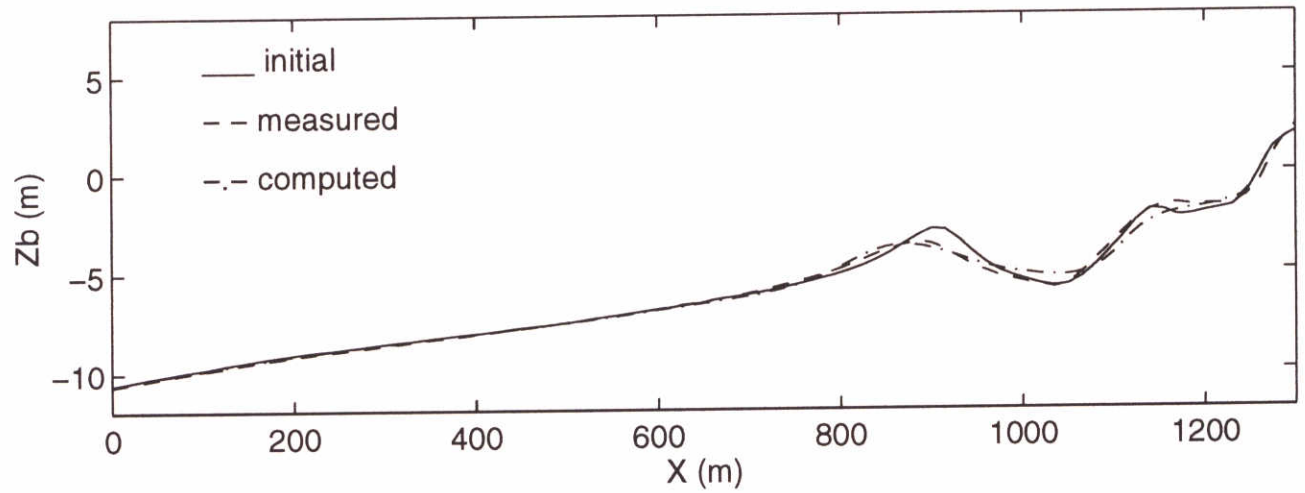

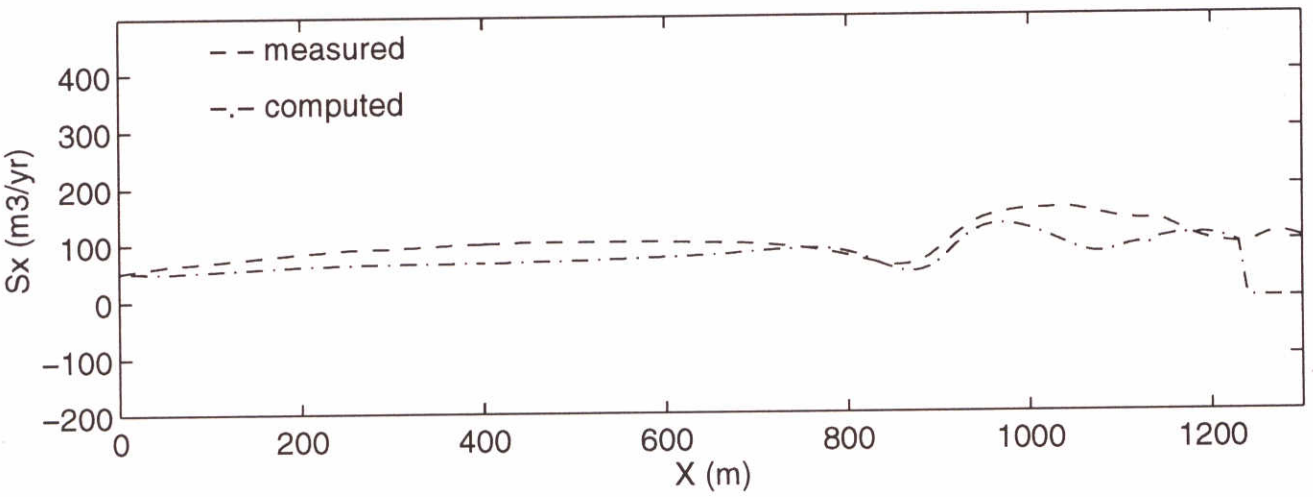

Comparison undisturbed profile upper panel: profile development after 254 days lower panel: yearly averaged sediment transport	NOURTEC	
DELFT HYDRAULICS	H1698	Fig 8

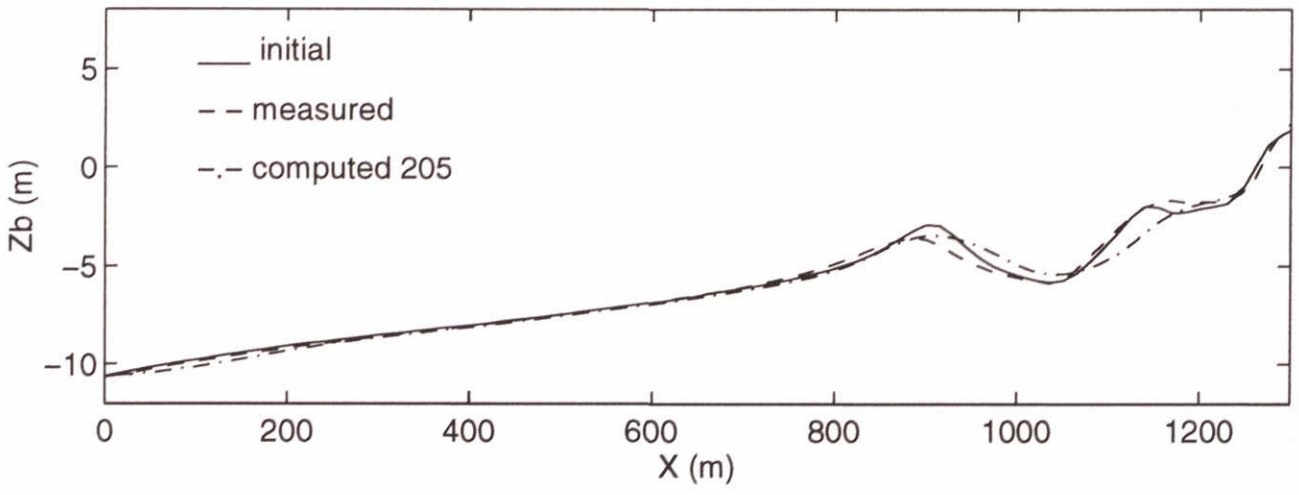

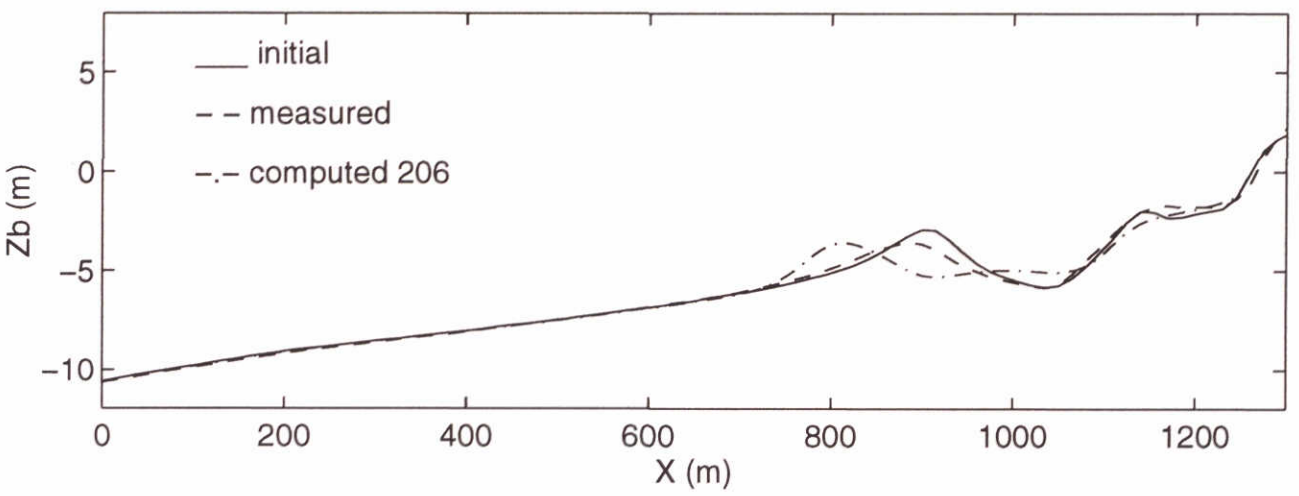

Comparison model vs. measurements
Wave breaking effects
autonomous profile after 254 days

NOURTEC

DELFT HYDRAULICS

H1698

Fig 9

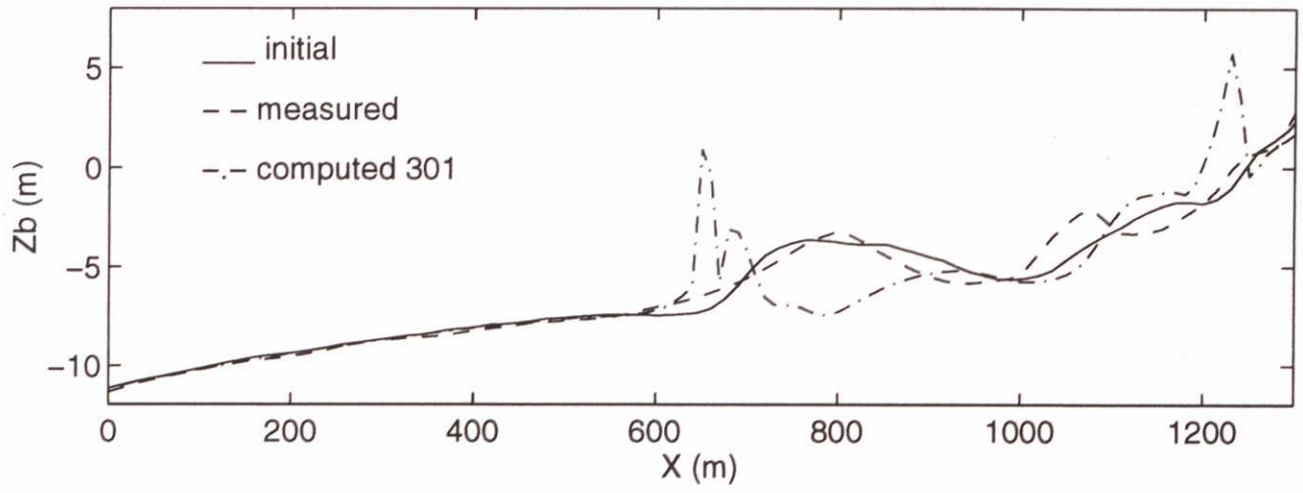

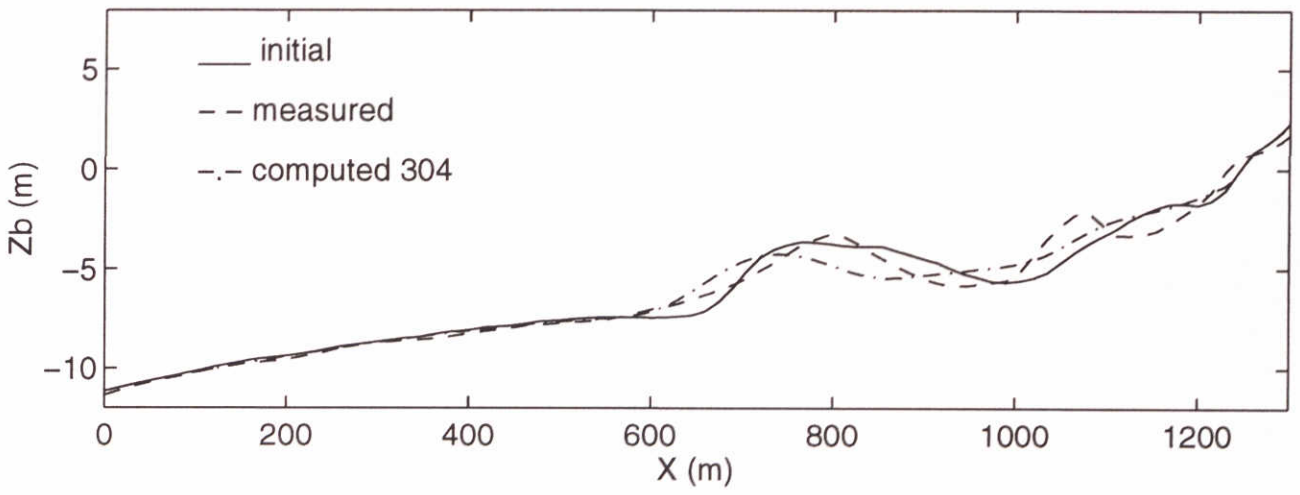

Comparison model vs. measurements
slope effect
nourished profile after 254 days

NOURTEC

DELFT HYDRAULICS

H1698

Fig 10

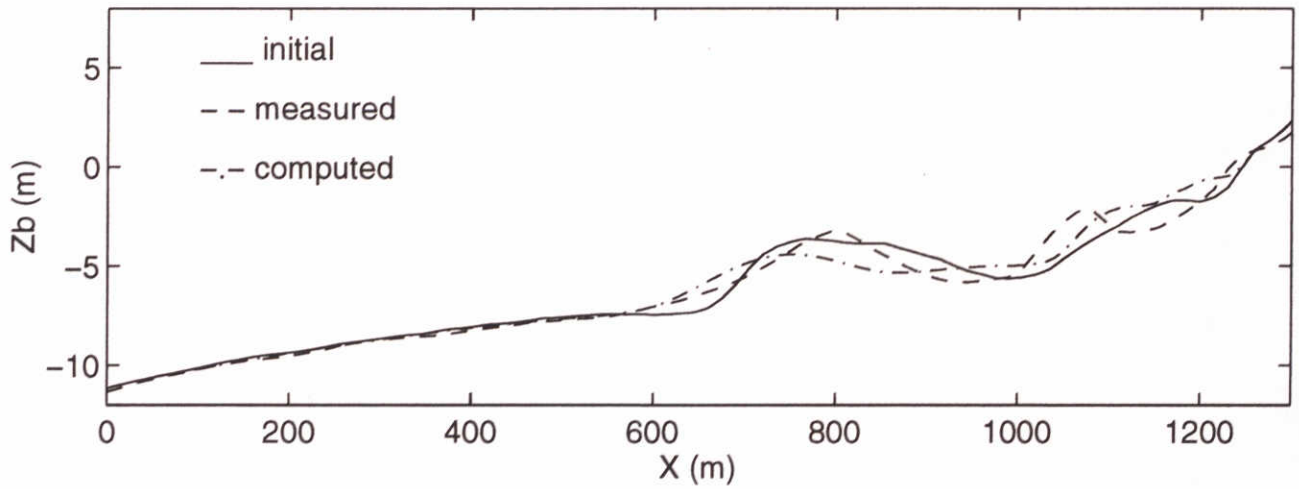

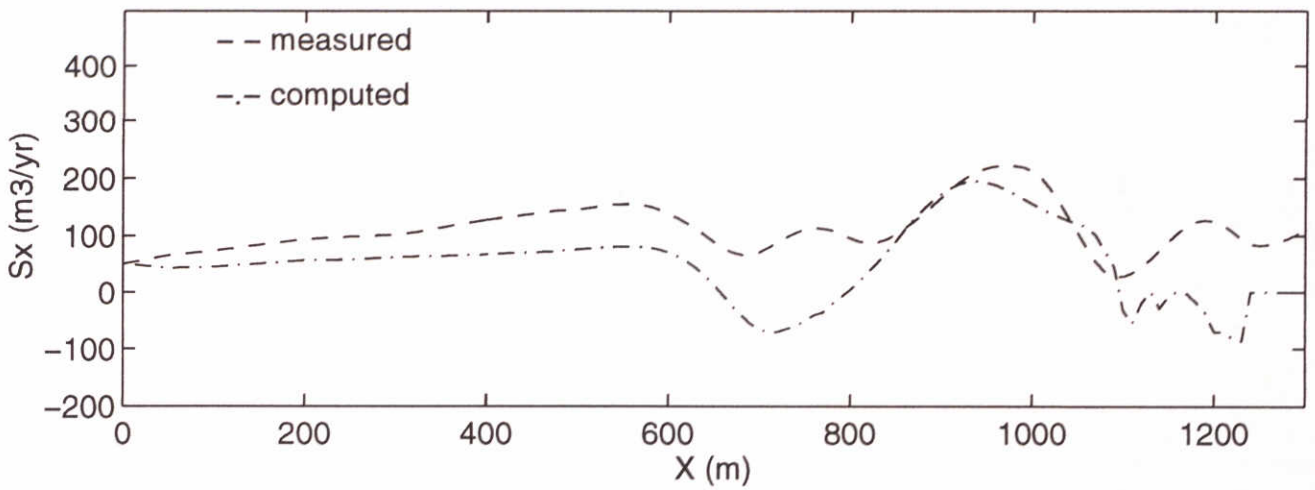

Comparison nourished profile
upper panel: profile development after 254 days
lower panel: yearly averaged sediment transport

NOURTEC

DELFT HYDRAULICS

H1698

Fig 11

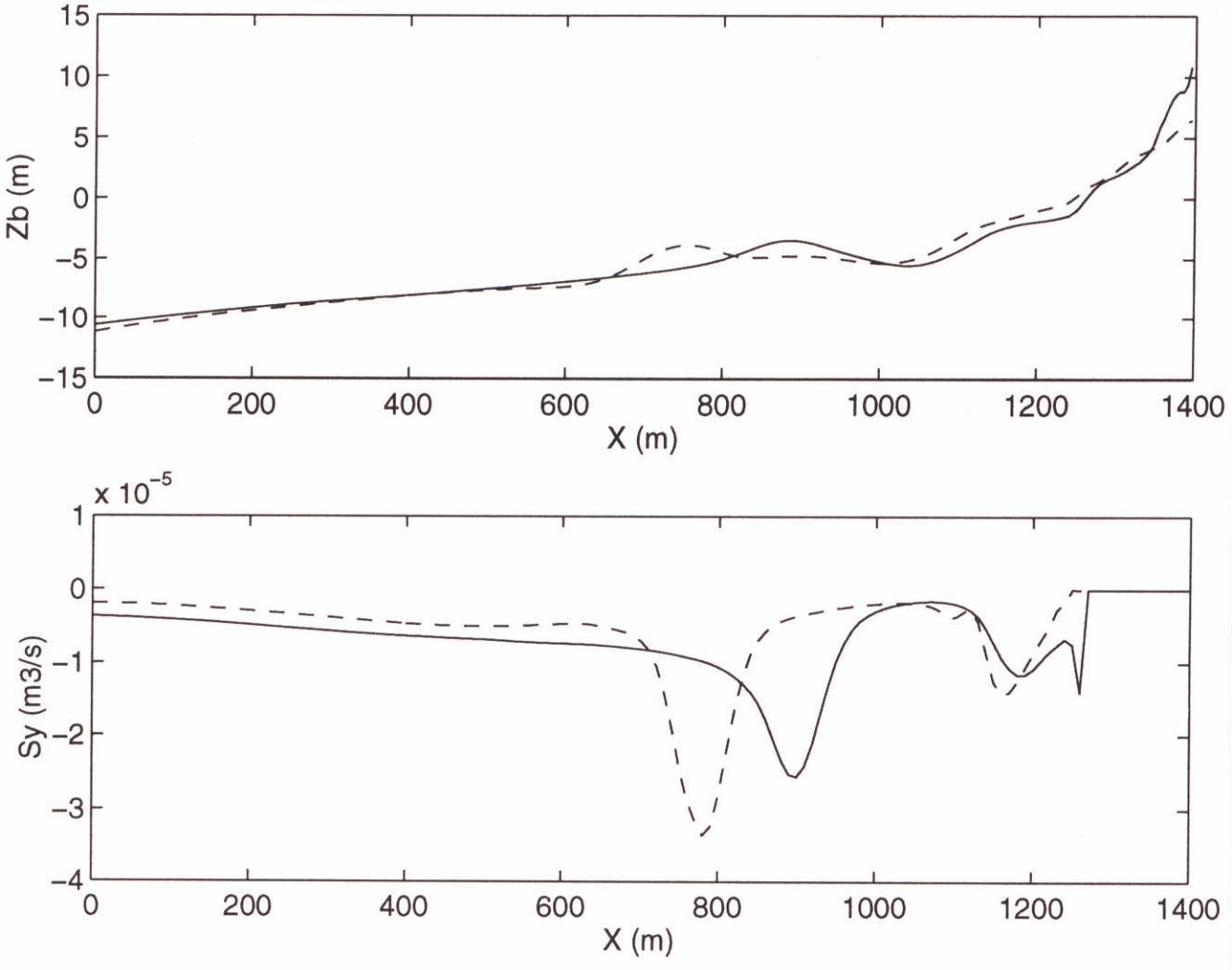

Alongshore sediment transport
upper panel: mean profiles
lower panel: average sediment transport

NOURTEC

DELFT HYDRAULICS

H1698

Fig 12

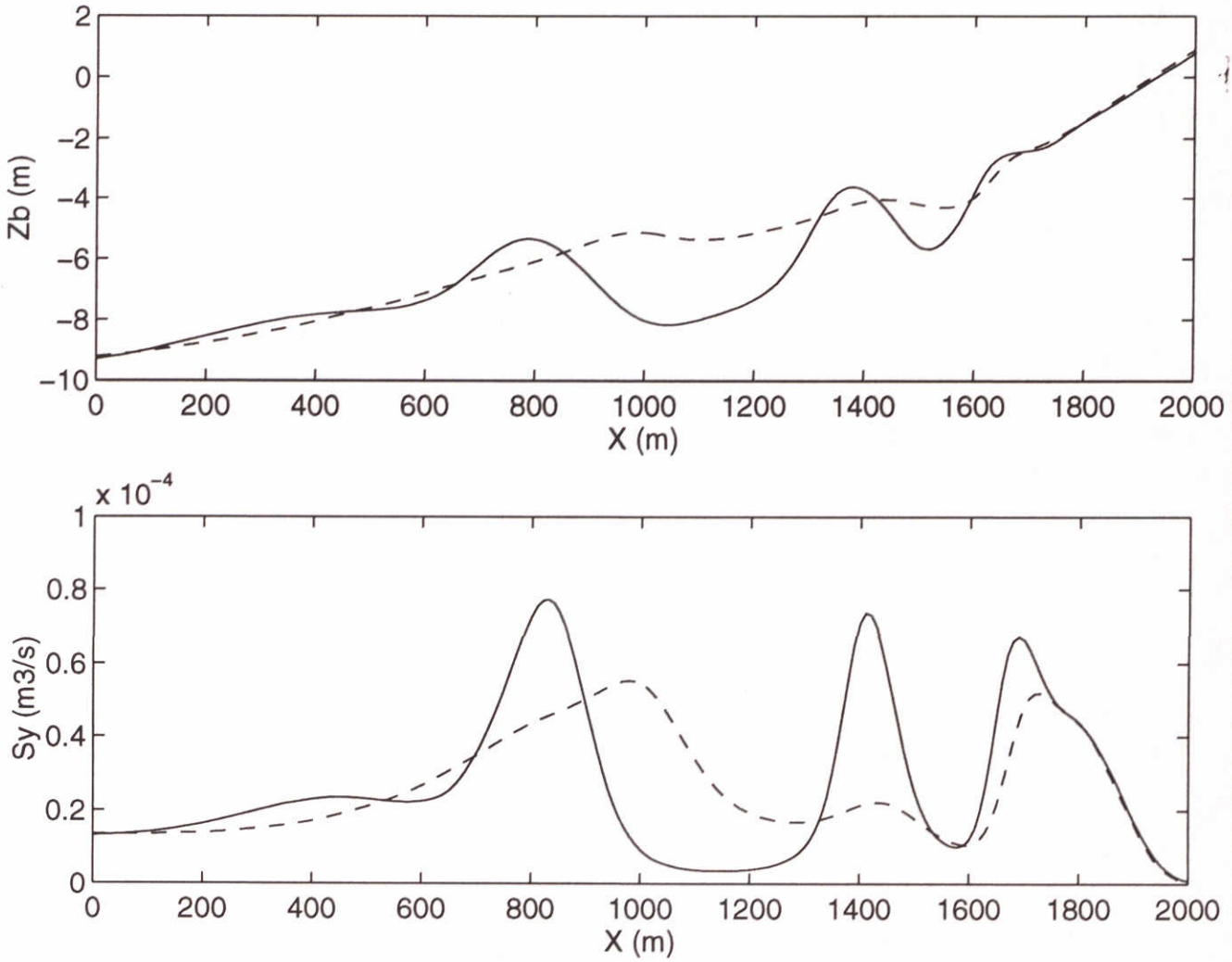

Alongshore sediment transport upper panel: mean profiles lower panel: average sediment transport	NOURTEC	
DELFT HYDRAULICS	H1698	Fig 13

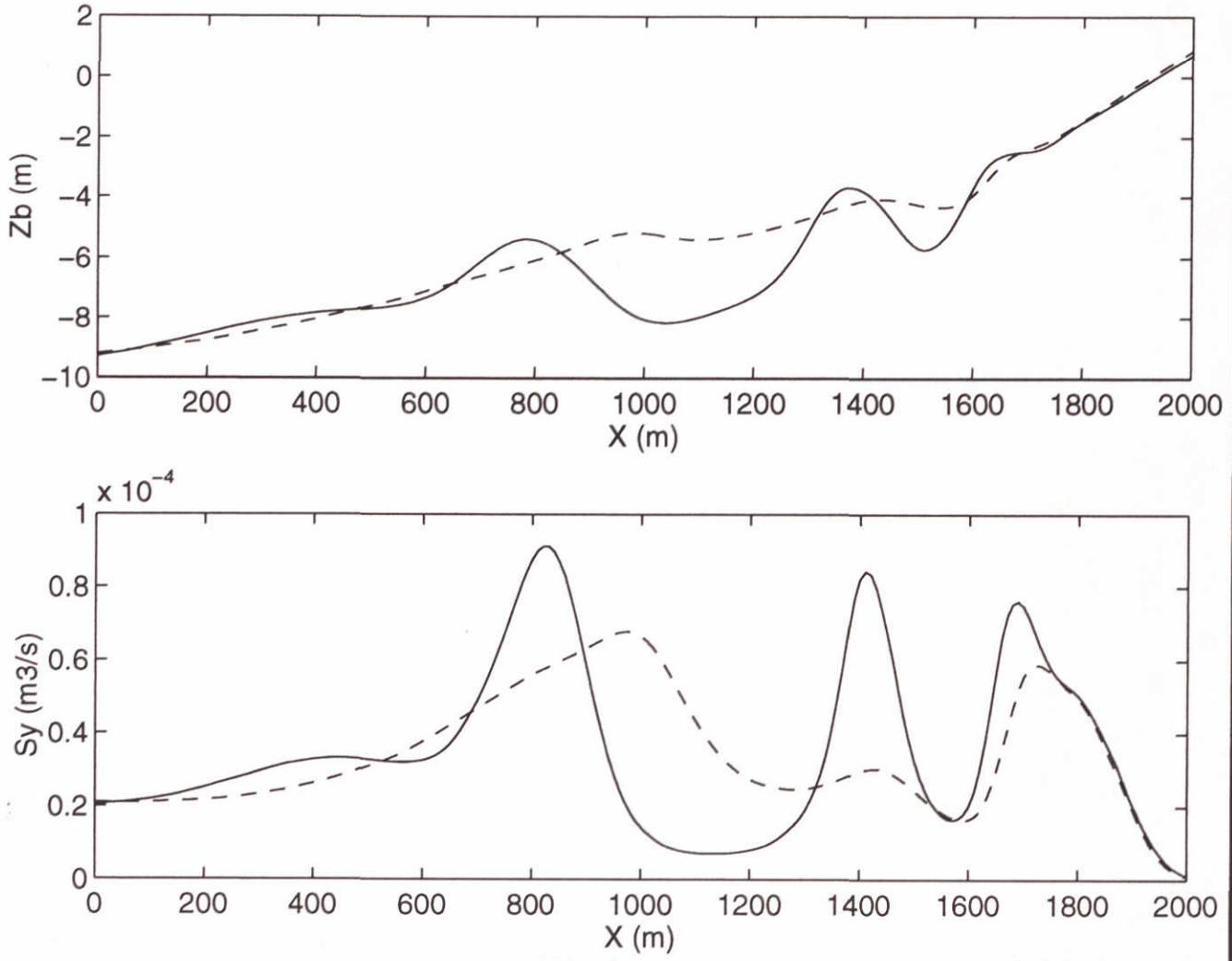

Alongshore sediment transport
upper panel: mean profiles
lower panel: average sediment transport

NOURTEC

DELFT HYDRAULICS

H1698

Fig 14

location Delft
Rotterdamseweg 185
p.o. box 177
2600 MH Delft
The Netherlands
telephone +31 15 569353
telefax + 31 15 619674
telex 38176 hydel-nl
e-mail info@wldelft.nl

As from October 10, 1995
telephone +31 15 2569353
telefax +31 15 2619674

location 'De Voorst'
Voorsterweg 28, Marknesse
p.o. box 152
8300 AD Emmeloord
The Netherlands
telephone +31 5274 2922
telefax +31 5274 3573
telex 42290 hylvo-nl
e-mail info@wldelft.nl

As from October 10, 1995
telephone +31 527 242922
telefax +31 527 243573